

RESEARCH ARTICLE

Investigating the outcomes of virus coinfection within and across host species

Ryan M. Imrie^{1*}, Sarah K. Walsh¹, Katherine E. Roberts¹, Joanne Lello², Ben Longdon¹

1 Centre for Ecology & Conservation, Faculty of Environment, Science, and Economy, Biosciences, University of Exeter, Penryn Campus, Penryn, United Kingdom, **2** School of Biosciences, Cardiff University, Cardiff, United Kingdom

* r.imrie@exeter.ac.uk



OPEN ACCESS

Citation: Imrie RM, Walsh SK, Roberts KE, Lello J, Longdon B (2023) Investigating the outcomes of virus coinfection within and across host species. PLoS Pathog 19(5): e1011044. <https://doi.org/10.1371/journal.ppat.1011044>

Editor: Ronald Swanstrom, University of North Carolina at Chapel Hill, UNITED STATES

Received: December 2, 2022

Accepted: May 2, 2023

Published: May 22, 2023

Copyright: © 2023 Imrie et al. This is an open access article distributed under the terms of the [Creative Commons Attribution License](https://creativecommons.org/licenses/by/4.0/), which permits unrestricted use, distribution, and reproduction in any medium, provided the original author and source are credited.

Data Availability Statement: All data underlying these findings is available at <https://doi.org/10.6084/m9.figshare.21657503.v1>.

Funding: The work described in our manuscript was funded by support from the following sources: BL, KER and RMI are supported by a Sir Henry Dale Fellowship jointly funded by the Wellcome Trust and the Royal Society (grant no. 109356/Z/15/Z), and a studentship funded by the Natural Environment Research Council (NERC) GW4+ Doctoral Training Partnership. SKW is funded by a studentship from the Biotechnology and Biological

Abstract

Interactions between coinfecting pathogens have the potential to alter the course of infection and can act as a source of phenotypic variation in susceptibility between hosts. This phenotypic variation may influence the evolution of host-pathogen interactions within host species and interfere with patterns in the outcomes of infection across host species. Here, we examine experimental coinfections of two *Cripaviruses*—Cricket Paralysis Virus (CrPV), and *Drosophila C Virus* (DCV)—across a panel of 25 *Drosophila melanogaster* inbred lines and 47 *Drosophilidae* host species. We find that interactions between these viruses alter viral loads across *D. melanogaster* genotypes, with a ~3 fold increase in the viral load of DCV and a ~2.5 fold decrease in CrPV in coinfection compared to single infection, but we find little evidence of a host genetic basis for these effects. Across host species, we find no evidence of systematic changes in susceptibility during coinfection, with no interaction between DCV and CrPV detected in the majority of host species. These results suggest that phenotypic variation in coinfection interactions within host species can occur independently of natural host genetic variation in susceptibility, and that patterns of susceptibility across host species to single infections can be robust to the added complexity of coinfection.

Author summary

The susceptibility of a host to infection can be influenced by the presence of co-occurring (i.e., coinfecting) pathogens, which can interact by suppressing and activating host immunity, and competing for host resources. The influence of coinfections on host susceptibility could have ramifications for the evolution of hosts and pathogens, and this may be seen within a single host species as a change in the contribution of host genetics to susceptibility during coinfections, and across host species as a change in the ability of evolutionary relationships to explain similarities in susceptibility. Here, we test these possibilities by measuring susceptibility to two different *Cripaviruses* during single infections and coinfections across different insect host genotypes and host species. We find that these two viruses interact during coinfections within the fruit fly *Drosophila melanogaster*, altering host susceptibility, but that variation in this interaction didn't show any evidence of being influenced by host genetics. Similarly, we find little evidence of the explanatory power of

Sciences Research Council (BBSRC) South West Biosciences Doctoral Training Partnership (BB/M009122/1). The funders had no role in study design, data collection and analysis, decision to publish, or preparation of the manuscript.

Competing interests: The authors have declared that no competing interests exist.

evolutionary relationships across host species changing between single infections and coinfections. These results suggest that variation in interactions between pathogens can occur without the influence of host genetics, and that it is possible for patterns in susceptibility across host species measured during single infection to be maintained during coinfection.

Introduction

Coinfections—simultaneous infections of a host with multiple pathogen lineages or species—are ubiquitous in nature, and represent the real-world context in which many infections occur [1–3]. Interactions between pathogens during coinfection can alter the virulence experienced by the host, and the loads and transmission rates of one or both pathogens [4–9]. At a population level, these interactions can lead to changes in infectious disease dynamics [10,11], such as the exclusion of novel viruses from host populations with other established pathogens [12,13], or fluctuations in the epidemic spread of one virus depending on the prevalence of other viruses [14,15]. These changes can ultimately alter the selective pressures imposed on hosts and pathogens, and coinfections have been proposed as a mechanism for the maintenance of genetic diversity in pathogen populations; as the fitness of pathogen genotypes may fluctuate not only in red queen dynamics with the host but also with coinfection prevalence and a pathogen's competitive ability across coinfection scenarios [16]. Despite this, coinfections remain a largely understudied source of phenotypic variation during infection, and further investigation of their influence on the outcome of infection in different hosts and host species is needed.

Within coinfecting hosts, pathogens can interact directly, such as through the production of toxins, modulation of the opposing pathogen's gene expression, and the production of hybrid virions [17–19], or indirectly through the production of common goods, competition for host resources, and interactions with host gene expression and immunity [20–25]. For example, in HIV-virus coinfections—a mechanistically well studied set of interactions due to their suspected involvement in AIDS progression [26]—several viruses have been shown to alter susceptibility to HIV infection by changing the expression of cell surface receptors CD4 and CCR5 [27,28]. In the case of human cytomegalovirus (HCMV), which upregulates CCR5 expression and increases HIV viral loads in coinfecting tissues, HIV can reciprocally induce the expression of transmembrane proteins that promote HCMV infection [29,30]. Conversely, measles virus coinfections can inhibit HIV-1 replication due to measles-related activation of proinflammatory cytokines [31]. As such, the presence of coinfecting viruses may enhance or interfere with the ability of a virus to effectively establish an infection in a host, with these interactions often mediated by host components.

Despite the known role of host components in many coinfections, the extent to which host genetic variation in these components can influence the strength of interactions between pathogens—and so the ability of hosts to evolve directly to selective pressures imposed by coinfection—is unknown. Evidence suggesting a role of host genetics in the outcomes of coinfections is limited; however, several studies in plants have shown that pathogen community composition, coinfection prevalence, and disease severity during coinfection can vary non-randomly between host genotypes [32–34]. Coinfections can also be influenced by host dietary choices and the quantity of nutrients available in the host [35,36]—both of which are heritable traits [37,38]—which suggests that host genetic variation may influence coinfection outcomes. Broadly, we may expect host genetic variation to lead to changes in the strength of interaction between coinfecting pathogens when the interaction occurs through modulation of a host

component (e.g., immune pathways or resource competition), or when host genetic variation influences the pathogen load of one or both pathogens.

Variation in the outcomes of coinfection across host species has also received relatively little attention, with most cross-species studies to date focusing either on single infections in controlled experimental systems [39–46] or looking for broad patterns in infections across large datasets of natural systems where coinfection status is unknown [47–53]. These studies have shown that the evolutionary relationships between host species can explain a large proportion of the variation in infection traits. For example, virulence tends to increase [46–48], and onward transmission and pathogen load decrease [40,47], with greater evolutionary distance between donor and recipient hosts. Irrespective of distance to the donor host, closely related species also tend to share similar levels of susceptibility to novel pathogens [40–42]. Phylogenetic models such as these form part of the growing field of zoonotic risk prediction, the aim of which is to provide accurate and actionable predictions of host-virus interactions to inform public health measures [54]. The accuracy of current models may be improved by identifying and incorporating additional sources of variation in the outcome of cross-species transmission [55]. Coinfection status, detectable through metagenomic screening [56], may be a beneficial inclusion in such models, provided the strength and/or direction of coinfection interactions are known (or inferable).

Here, we investigate the influence of coinfection on virus susceptibility within and across host species, using panels of *Drosophila* hosts and experimental infections with two *Cripa-viruses*: Cricket Paralysis Virus (CrPV) and *Drosophila* C Virus (DCV). Viral loads were measured during single and coinfection conditions across 25 inbred lines of *Drosophila melanogaster* and 47 *Drosophilidae* species. By analysing both viral loads and the change in viral loads from single to coinfection, we quantify the host genetic and phylogenetic components of susceptibility to each virus, and investigate whether these host components also influence the strength and direction of coinfection interactions in this system.

Both DCV and CrPV are well studied pathogens in *Drosophila melanogaster* and multiple similarities exist in their interactions with their hosts that could lead to interactions during coinfection. Both viruses are targeted by the antiviral RNAi pathway during infection of *D. melanogaster* [57,58], and activate the IMD immune signalling pathway, inducing nonspecific antiviral gene expression [59–61]. Each encodes an inhibitor of antiviral RNAi, which act on different components of the pathway; the DCV inhibitor binds and sequesters viral RNA to prevent its cleavage by the antiviral RNAi endonuclease *Dicer-2*, and also disrupts formation of the RNA-induced silencing complex (RISC) [62,63]; the CrPV inhibitor binds the RISC protein *Argonaute-2*, causing suppression of RISC viral RNA cleavage [63]. Infections with DCV have also been shown to induce nutritional stress in infected hosts, due to intestinal obstruction and accumulation of food in the fly crop, although CrPV infection results in no such phenotype [64]. DCV and CrPV may therefore be capable of interacting indirectly during coinfection through multiple routes: by suppression of antiviral RNAi, transactivation of host antiviral gene expression, or competition for limited host resources. As such, coinfection could enhance the accumulation of one or both viruses by suppressing host immunity. Alternatively, coinfection may result in lower titres for one or both viruses due to activation of general antiviral immune responses or competition for host resources.

Susceptibility to DCV infection has a strong host genetic component [65], with polymorphisms in two major-effect genes (*pastrel* and *Ubc-E2H*) explaining a large proportion of the variation in DCV susceptibility [65–68]. Both genes have also been implicated in CrPV susceptibility during knockdown experiments [68]. DCV and CrPV both vary widely in their ability to persist and replicate across different *Drosophilidae* host species, and are strongly positively correlated in their susceptibilities across host species [42]. For both viruses, the host phylogeny

explained a large proportion of the variation in viral load during single infection [41–43,45]. A role of host genetics during coinfection may therefore manifest either as a change in the genetic or phylogenetic components of susceptibility to each individual virus, or as a genetic or phylogenetic component directly influencing the strength of interaction between these viruses. We tested the possibility that host genetic or phylogenetic components can influence the outcomes of coinfection in two separate experiments that measured viral loads of DCV and CrPV in both single and coinfection settings across two different host panels. In the first experiment, we examined the differences between single and coinfection viral loads across different host genotypes within-species, using 25 inbred lines of *Drosophila melanogaster* from the *Drosophila* Genetic Reference Panel (DGRP) [69]. In the second experiment, we examined differences across-species using 47 *Drosophilidae* host species.

Materials & methods

Fly stocks

Stocks of DGRP flies were kindly provided by Jon Day and Francis Jiggins [65]. In total, 25 DGRP lines were used (for details see S1 Table), with 15 lines containing the resistant “G” allele of the A2469G *pastrel* SNP and 10 containing the susceptible “A” allele [66]. *Pastrel* allele status was confirmed via conventional PCR using SNP genotyping primers from [66] (S2 Table). Laboratory stocks of 47 *Drosophilidae* host species were used to provide the across-species host panel (S3 Table), as in previous studies [41,42].

All flies were maintained in multi-generation stock bottles (Fisherbrand) at 22°C, 70% relative humidity in a 12-hour light-dark cycle. Each stock bottle contained 50ml of one of four varieties of *Drosophila* media (<https://doi.org/10.6084/m9.figshare.21590724.v1>) which were chosen to optimise rearing conditions for parental flies. All fly lines and species were confirmed to be negative for infection with CrPV and DCV prior to experiments by quantitative reverse-transcription PCR (qRT-PCR, described below). To limit the effects of variation in larval density on the condition of DGRP lines, experimental flies were reared in vials with finite numbers of larvae, achieved by transferring groups of five 7 day old mated females to fresh vials each day for 3 days, with daily pools of offspring from these vials collected for experiments. Due to large differences in fecundity, larval density controls were not practical for the across-species host panel.

Inferring the *Drosophilidae* host phylogeny

The method used to infer the host phylogeny has been described in detail elsewhere [41]. Briefly, publicly available sequences of the 28S, *Adh*, *Amyrel*, *COI*, *COII*, *RpL32*, and *SOD* genes were collected from Genbank (see <https://doi.org/10.6084/m9.figshare.13079366.v1> for a full breakdown of genes and accessions by species). Gene sequences were aligned in Geneious version 9.1.8 (<https://www.geneious.com>) using a progressive pairwise global alignment algorithm with free end gaps and a 70% similarity IUB cost matrix. Gap open penalties, gap extension penalties, and refinement iterations were kept as default.

Phylogenetic reconstruction was performed using BEAST version 1.10.4 [70] as the subsequent phylogenetic mixed model (described below) requires a tree with the same root-tip distances for all taxa. Genes were partitioned into separate ribosomal (28S), mitochondrial (*COI*, *COII*), and nuclear (*Adh*, *Amyrel*, *RpL32*, *SOD*) groups. The mitochondrial and nuclear groups were further partitioned into groups for codon position 1+2 and codon position 3, with unlinked substitution rates and base frequencies across codon positions. Each group was fitted to separate relaxed uncorrelated lognormal molecular clock models using random starting trees and four-category gamma-distributed HKY substitution models. The BEAST analysis

was run twice, with 1 billion Markov chain Monte Carlo (MCMC) generations sampled every 100,000 iterations, using a birth-death process tree-shape prior. Model trace files were evaluated for chain convergence, sampling, and autocorrelation using Tracer version 1.7.1 [71]. A maximum clade credibility tree was inferred from the posterior sample with a 10% burn-in. The reconstructed tree was visualised using ggtree version 2.0.4 [72].

Virus isolates

Virus stocks were kindly provided by Julien Martinez (DCV) [73], and Valérie Dorey and Maria Carla Saleh (CrPV) [62]. The DCV isolate used here (DCV-C) was isolated from lab stocks established by wild capture in Charolles, France [74], and the CrPV isolate was collected from *Teleogryllus commodus* in Victoria, Australia [75]. Virus stocks were checked for contamination with CrPV (DCV) and DCV (CrPV) by qRT-PCR and diluted in Ringers solution [76] to equalise the relative concentrations of viral RNA. Before inoculation, virus aliquots were either mixed 1:1 with Ringers (single infection inoculum) or 1:1 with an aliquot of the other virus (coinfection inoculum). This was done to keep the individual doses of each virus consistent between infection conditions.

Inoculation

Before inoculation, 0–1 day old male flies were transferred to vials containing cornmeal media. These flies were then transferred to fresh media every 2 days for a week (age 7–8 days), at which point they were inoculated. Vials contained between 7 and 20 flies (mean = 12.7), and were kept at 22°C, 70% relative humidity in a 12-hour light-dark cycle throughout the experiments. Male flies were used to avoid any effect of sex or mating status, which has been shown to influence the susceptibility of female flies to other pathogens [77–79]. Flies were inoculated under CO₂ anaesthesia via septic pin prick with 12.5µm diameter stainless steel needles (Fine Science Tools, CA, USA). These needles were bent approximately 250µm from the end to provide a depth stop and dipped in virus inoculum before being pricked into the pleural suture of anaesthetised flies. Inoculation by this method bypasses the gut immune barrier but avoids differences in inoculation dose due to variation in feeding rate, and infections using this route largely follow the same course as oral infections but with less stochasticity [80].

Measuring change in viral load

To provide a measure of viral load during single and coinfection, inoculated flies were snap frozen in liquid nitrogen at 2 days (\pm 2 hours) post-inoculation. Additional samples were collected for each species in the *Drosophilidae* host panel immediately after inoculation, which were used to account for differences in housekeeping gene expression across host species during C_T normalisation (see below). Total RNA was extracted from flies homogenized in Trizol (Invitrogen) using chloroform-isopropanol extraction, and reverse transcribed using GoScript reverse transcriptase (Promega) with random hexamer primers. qRT-PCR was carried out on 1:2 diluted cDNA on an Applied Biosystems StepOnePlus system using a Sensifast Hi-Rox SYBR kit (Bioline). Cycle conditions were as follows: initial denaturation at 95°C for 120 seconds, then 40 cycles of 95°C for 5 seconds and 60°C for 30 seconds. The primer pairs used for virus qRT-PCR assays were: (DCV) forward, 5'-GACACTGCCTTTGATTAG-3'; reverse, 5'-CCCTCTGGGAAGTAAATG-3'; (CrPV) forward, 5'-TTGGCGTGGTAGTATGCGTAT-3'; reverse, 5'-TGTTCCGTCCTGCGTCTC. RPL32 housekeeping gene primers were used for normalisation and varied by species (S4 and S5 Tables). For each biological sample, two technical replicate qRT-PCR reactions were performed for each amplicon (viral and RPL32).

Between-plate variation in C_T values was estimated and corrected using linear models with plate ID and biological replicate ID as fixed-effects [81,82]. For DGRP lines, mean viral C_T values from technical replicate pairs were normalised to RPL32 and converted to relative viral load using the $\Delta\Delta C_T$ method, where $\Delta C_T = C_{T:\text{Virus}} - C_{T:\text{RPL32}}$ and $\Delta\Delta C_T = 40 - \Delta C_T$. To account for potential differences in RPL32 expression between species, change in viral load in the *Drosophilidae* species experiment was calculated as fold-change in viral load from inoculation to 2 days post-infection using the $\Delta\Delta C_T$ method, where $\Delta C_T = C_{T:\text{Virus}} - C_{T:\text{RPL32}}$ and $\Delta\Delta C_T = \Delta C_{T:\text{day0}} - \Delta C_{T:\text{day2}}$. Amplification of the correct products was verified by melt curve analysis. Repeated failure to amplify product, the presence of melt curve contaminants, or departures from the melt curve peaks of positive samples ($\pm 1.5^\circ\text{C}$ for viral amplicons; $\pm 3^\circ\text{C}$ for RPL32) were used as exclusion criteria for biological replicates. For a full breakdown of the replicates per experiment for each combination of fly line/species and infection condition see [S6 Table](#).

Analysis of coinfection within and across species

Genetic variation in the outcome of single and coinfection across DGRP lines was analysed using methods previously described by Magwire et al. [65]. Briefly, multivariate generalised linear mixed models (GLMMs) were fitted using the R package MCMCglmm [83], with either the viral loads of each virus under each infection condition, or the change in viral load during coinfection (coinfection viral load—single infection viral load) as the response variable. The structures of these models were as follows:

$$y_{lic} = \beta_{1:c} + \mu_{l:c} + \mu_{b:c} + e_{lic} \quad (1)$$

$$y_{liv} = \beta_{1:v} + \mu_{l:v} + \mu_{b:v} + e_{liv} \quad (2)$$

In model (1), y_{lic} is the viral load for the combination of virus and infection condition c (CrPV single infection, CrPV coinfection, DCV single infection, DCV coinfection) in the i^{th} biological replicate of DGRP line l . The fixed effect β_l represents the intercepts for each combination, the random effect μ_l represents the deviation of each DGRP line from the overall mean viral load for each combination (equivalent to the between-line variance), and e_{lic} represents the residual error. A small but significant effect of experiment block was found in initial models, driven by ~10 fold differences in DCV viral loads of the third experimental block. To account for this, random effects of block by infection condition ($\mu_{b:c}$, $\mu_{b:v}$) were added to both models. The structure of model (2) remains the same, but with the change in viral load during coinfection for each virus as the response variable, and y_{liv} representing the change in viral load for the i^{th} biological replicate of virus v and DGRP line l . *Pastrel* allele status (susceptible “A”, resistant “G”) was included in additional models as a fixed effect ($\beta_{2:lp}$).

Phylogenetic GLMMs were used to investigate the effects of host evolutionary relatedness on viral load during single and coinfection, and to calculate interspecific correlations between different infection conditions across host species. Multivariate models were fitted with the viral loads of each virus under each infection condition as the response variable. The structure of these models were as follows:

$$y_{hic} = \beta_{1:c} + \mu_{p:hc} + \mu_{s:hc} + e_{hic} \quad (3)$$

$$y_{hic} = \beta_{1:c} + \mu_{p:hc} + e_{hic} \quad (4)$$

In these models, y_{hic} is the change in viral load for the combination of virus and infection condition c (CrPV single infection, CrPV coinfection, DCV single infection, or DCV coinfection) in the i^{th} biological replicate of host species h . The fixed effect β_l represents the intercepts

for each combination, the random effect μ_p represents the effects of the host phylogeny assuming a Brownian motion model of evolution, and e represents the model residuals. Model (3) also includes a species-specific random effect that is independent of the host phylogeny ($\mu_{s:hc}$). This explicitly estimates the non-phylogenetic component of between-species variance and allows the proportion of variance explained by the host phylogeny to be calculated. $\mu_{s:hc}$ was removed from model (4) as model (3) struggled to separate the phylogenetic and species-specific traits for some infection conditions. Wing size, measured as the length of the IV longitudinal vein from the tip of the proximal segment to the join of the distal segment with vein V [84], provided a proxy for body size [85] and was included in a further model as a fixed effect ($wingsize\beta_{2:hc}$). This was done to ensure that any phylogenetic signal in body size did not explain the differences seen in viral load between species [86].

To investigate the effect of host genetics and host evolutionary relatedness on the change in viral load from single to coinfection, additional models were run with the change in viral load during coinfection (coinfection viral load—single infection viral load) on viral load as the response variable:

$$y_{hiv} = \beta_{1:v} + \mu_{p:hv} + \mu_{s:hv} + e_{hiv} \quad (5)$$

$$y_{hiv} = \beta_{1:v} + \mu_{p:hv} + e_{hiv} \quad (6)$$

In these models, y_{hiv} is the change in viral load for the i^{th} biological replicate of virus v and host genotype or species h . The explanatory structure otherwise remains the same as models (3–4).

Within models (1–6), the random effects and residuals were assumed to follow a multivariate normal distribution and a centred mean of 0. Models (1–2) were fitted with a covariance structure $V_t \otimes I$ for the between line variances, and $V_e \otimes I$ for the residuals, with \otimes representing the Kronecker product, and I representing an identity matrix. V represents 4 x 4 covariance matrices for model (1) and 2 x 2 covariance matrices for model (2) which describe the between-line variances and covariances in viral load for each infection condition and virus. Models (3–6) were fitted with a covariance structure of $V_p \otimes A$ for the phylogenetic effects, $V_s \otimes I$ for species-specific effects, and $V_e \otimes I$ for residuals. A represents the host phylogenetic relatedness matrix, I an identity matrix, and V represents 4 x 4 covariance matrices for models (3–4), or 2 x 2 covariance matrices for models (5–6), describing the between-species variances and covariances of changes in viral load for each combination of virus and infection condition. As each biological replicate was only tested with one combination of virus and infection condition, the covariances of V_e cannot be estimated and were set to 0 for all models.

Models were run for 13 million MCMC generations, sampled every 5000 iterations with a burn-in of 3 million generations. Parameter expanded priors were placed on the covariance matrices, resulting in multivariate F distributions with marginal variance distributions scaled by 1000. Inverse-gamma priors were placed on the residual variances, with a shape and scale equal to 0.002. To ensure the model outputs were robust to changes in prior distribution, models were also fitted with flat and inverse-Wishart priors, which gave qualitatively similar results. All parameter estimates reported from models (1–6) are means of the posterior density, and 95% credible intervals (CIs) are the 95% highest posterior density intervals which are reported in brackets following the estimates in the results.

The covariance matrices of models (1) and (2) were used to calculate the heritabilities (h^2), and covariates of additive genetic and environmental variation (CV_A and CV_E respectively) of viral load and the effects of coinfection within host species. Heritability was calculated as $h^2 = \frac{V_A}{V_A + V_E}$, where V_A represents the additive genetic variance and V_E the environmental

variance of each trait [87]. As DGRP lines are homozygous, V_A can be calculated as half the between-line variance, assuming purely additive genetic variation [65]. V_E was set as the residual variance of each model, which contains both non-additive genetic and environmental effects on viral load and any measurement errors. Genetic correlations between infection conditions were calculated from the model (1) and (2) v_l matrices as $\frac{cov_{x,y}}{\sqrt{var_x * var_y}}$ and slopes of each relationship as $\frac{cov_{x,y}}{var_x}$.

The proportion of the between species variance that can be explained by the phylogeny was calculated from models (3) and (5) using the equation $\frac{V_p}{V_p + V_s}$, where v_p and v_s represent the phylogenetic and species-specific components of between-species variance respectively [86], and are equivalent to phylogenetic heritability or Pagel's lambda [88,89]. The repeatability of viral load measurements was calculated from models (4) and (6) as $\frac{V_p}{V_p + V_e}$, where v_e is the residual variance of the model [90]. Interspecific correlations in viral load between single and coinfection were calculated from model (4) v_p matrix as $\frac{cov_{x,y}}{\sqrt{var_x * var_y}}$.

Results

Coinfection causes changes in DCV and CrPV viral load across *D. melanogaster* genotypes

To investigate variation in the outcome of coinfection within host species, we injected a total of 8,618 flies from 25 lines of the *Drosophila* Genetic Reference Panel with one of three virus inoculums: DCV, CrPV, and DCV + CrPV, and measured the outcome of infection as the viral load of each virus at 2 days post-inoculation using qRT-PCR (Fig 1). Point estimates of the mean viral load across lines suggest that DCV viral load increases ~3-fold during coinfection with CrPV, and CrPV viral load decreases ~2.5-fold during coinfection with DCV, although credible intervals of these estimates overlapped (Table 1, “Single Infection” and “Coinfection” conditions). When models were fitted on the change in viral load (coinfection-single infection), in effect treating viral loads within experiment blocks as paired data, similar and significant effects of coinfection across lines were detected (Table 1, “Change” conditions). Several lines showed notably large changes during coinfection: two DGRP lines showed ~10 fold decreases in CrPV viral load, and three lines showed ~40–150 fold increases in DCV viral load. Removing these lines from model (2) reduced the mean changes in viral load during coinfection to a ~2 fold increase for DCV and a ~2 fold decrease for CrPV, but the effects of coinfection on both viruses remained significant.

No evidence of a host genetic component to the outcome of coinfection

To estimate the influence of host genetic variation on the viral loads measured during single and coinfection, GLMMs were fitted to allow the phenotypic variation in viral loads to be partitioned into genetic and environmental components. Point estimates of heritability of DCV viral load (0.25–0.30) were higher than for CrPV (0.13), and this difference was driven by changes in the genetic component of variation (S7 Table): CrPV $CV_A = 0.08$, (0.05, 0.11), DCV $CV_A = 0.16$, (0.12, 0.20). This is consistent with previous studies which also found the genetic component of variation in susceptibility of *D. melanogaster* to single infections with DCV (a natural pathogen) is higher than for a novel pathogen [65]. However, we found little evidence that heritability of DCV or CrPV viral loads change in relation to coinfection, with the credible intervals of h^2 estimates for single and coinfection viral loads overlapping for both viruses (Table 1). Additionally, no host genetic component was found for the change in viral load

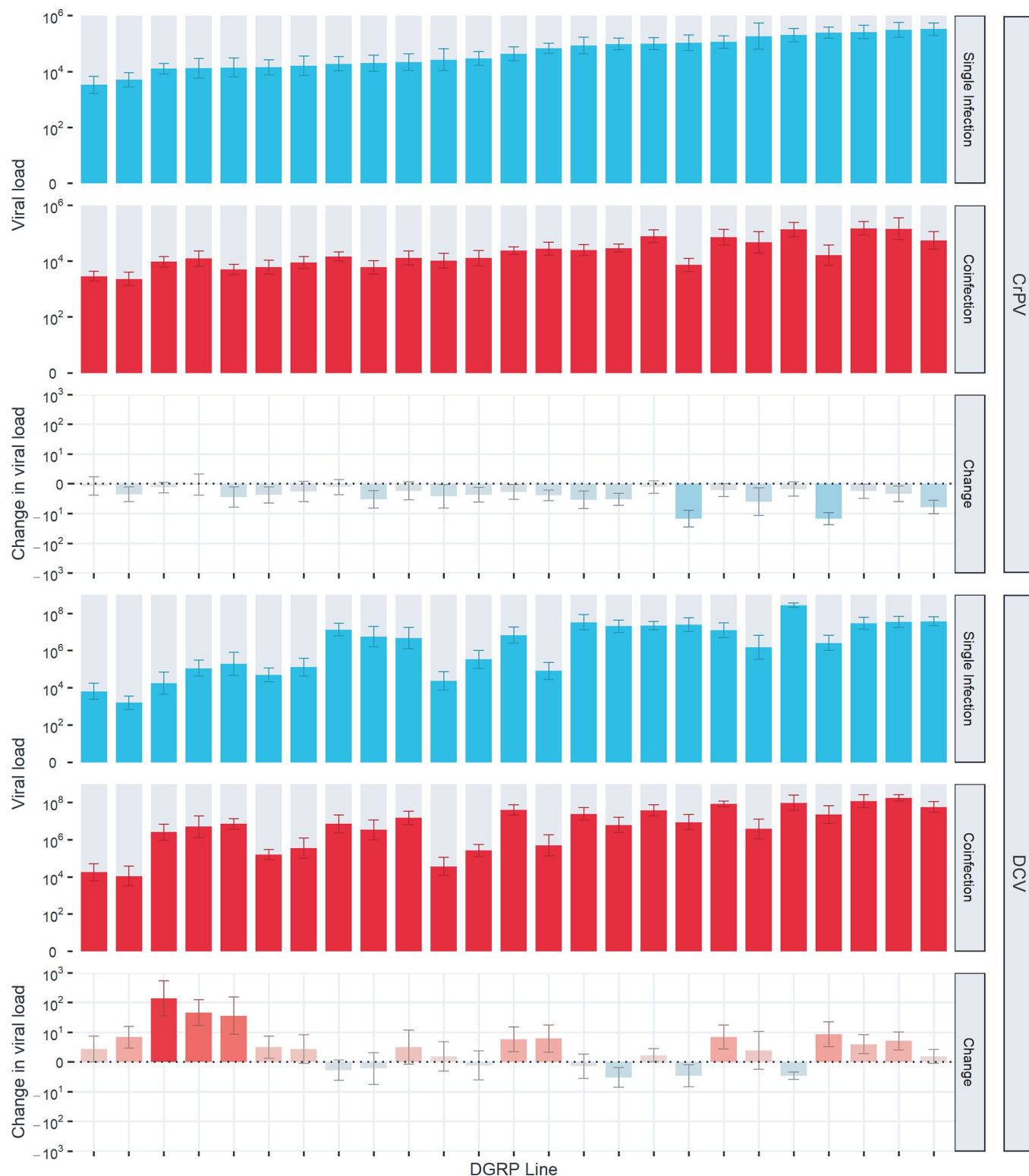


Fig 1. Viral loads of CrPV and DCV across DGRP lines during single and coinfection. Bar heights show the mean viral load or changes in viral load (coinfection-single infection) at 2 dpi on a log₁₀ scale, with error bars showing the standard error of the mean. Blue bars represent single infection viral loads, or changes in viral load where single infection viral loads were greater than coinfection viral loads. Red bars represent coinfection viral loads, or changes in viral load where coinfection viral loads were greater than single infection viral loads. DGRP lines are arranged on the x-axis in order of susceptibility to CrPV during single infection.

<https://doi.org/10.1371/journal.ppat.1011044.g001>

Table 1. Estimates of the phenotypic mean, environmental variance (V_E), additive genetic variance (V_A), and heritability (h^2) of viral load and the change in viral load during coinfection across DGRP lines for CrPV and DCV during single infection and coinfection. Values for “single infection” and “coinfection” conditions were taken from model (1), which was fitted on \log_{10} -transformed fold-changes in viral load, while values for “change” were taken from model (2), which was fitted on \log_{10} -transformed Δ fold-changes in viral load (coinfection-single infection).

Virus	Condition	Mean	V_E	V_A	h^2
CrPV	Single Infection	4.68 (4.02, 5.34)	0.94 (0.79, 1.09)	0.14 (0.05, 0.25)	0.13 (0.05, 0.22)
	Coinfection	4.28 (3.60, 4.96)	0.74 (0.61, 0.86)	0.12 (0.04, 0.20)	0.13 (0.06, 0.22)
	Change	-0.27 (-0.37, -0.18)	0.39 (0.05, 0.92)	0.00 (0.00, 0.02)	0.02 (0.00, 0.09)
DCV	Single Infection	6.17 (5.29, 6.98)	2.08 (1.75, 2.46)	1.00 (0.47, 1.65)	0.32 (0.20, 0.46)
	Coinfection	6.62 (5.82, 7.40)	1.80 (1.49, 2.09)	0.71 (0.33, 1.18)	0.28 (0.16, 0.40)
	Change	0.33 (0.18, 0.47)	0.21 (0.15, 0.27)	0.03 (0.00, 0.06)	0.11 (0.00, 0.23)

<https://doi.org/10.1371/journal.ppat.1011044.t001>

during coinfection (Tables 1 and S8). Together, this suggests that variation in the strength of coinfection interactions between these viruses was independent of natural host genetic variation, and that coinfection status does not appear to alter the host genetic component of susceptibility to either virus.

Correspondingly, strong positive correlations between single and coinfection viral loads were found for both DCV: $r = 0.94$ (0.84, 1.00), and CrPV: $r = 0.90$ (0.73, 1.00), with little evidence of genotype-by-coinfection interactions. Strong positive correlations were also seen between the two viruses, such that DGRP lines more susceptible to DCV were often also more susceptible to CrPV (Fig 2A–2D). No correlation was seen between the viral load of each virus during coinfection and the change in viral load between single and coinfection experienced by the other virus (S1 Fig), indicating that the strength of coinfection interaction between DCV and CrPV across *D. melanogaster* genotypes is not virus density dependent. Together, this suggests that susceptibility to DCV and CrPV share similar genetic architectures within *D. melanogaster*, with host genetic variation affecting DCV viral load similarly affecting CrPV viral load irrespective of coinfection status.

Viral load remains a repeatable trait across host species during coinfection

To investigate how coinfection may alter susceptibility across host species, we performed similar experimental single and coinfections across 47 *Drosophilidae* host species. A total of 13,596 flies were inoculated, and the change in viral load after two days of infection was measured by qRT-PCR (Fig 3). Neither virus showed evidence of changes in their overall mean viral loads or variance across host species between single and coinfection (Table 2). Power analysis based on the effects of coinfection found in *D. melanogaster* (Fig 1 and S1 Methods) showed that the level of replication in this experiment was adequate to detect systematic ~2-fold changes in viral load across host species. As such, this result suggests there is no evidence for large additive effects of coinfection that are consistent across host species. Instead, most host species showed no discernible differences in viral loads during coinfection, with notable exceptions including *D. obscura* (both viruses decreased in viral load by ~600 fold), *D. suzukii* (DCV unchanged but CrPV decreased by ~25 fold), *Zaprionus tuberculatus* (CrPV unchanged but DCV decreased by ~50 fold), and *D. virilis* (CrPV unchanged but DCV increased by ~40 fold).

Phylogenetic GLMMs were fitted to the data to determine the proportion of variation in viral load explained by the host phylogeny (Table 2). The host phylogeny explained a large proportion of the variation in viral load for CrPV during single infection: 0.88 (0.69, 1), and coinfection: 0.82 (0.59, 1), with no credible difference between these two estimates. Estimates of the variation in DCV viral load explained by phylogeny were low: 0.1–0.13 with wide credible intervals due to model (3) struggling to separate phylogenetic and non-phylogenetic effects for

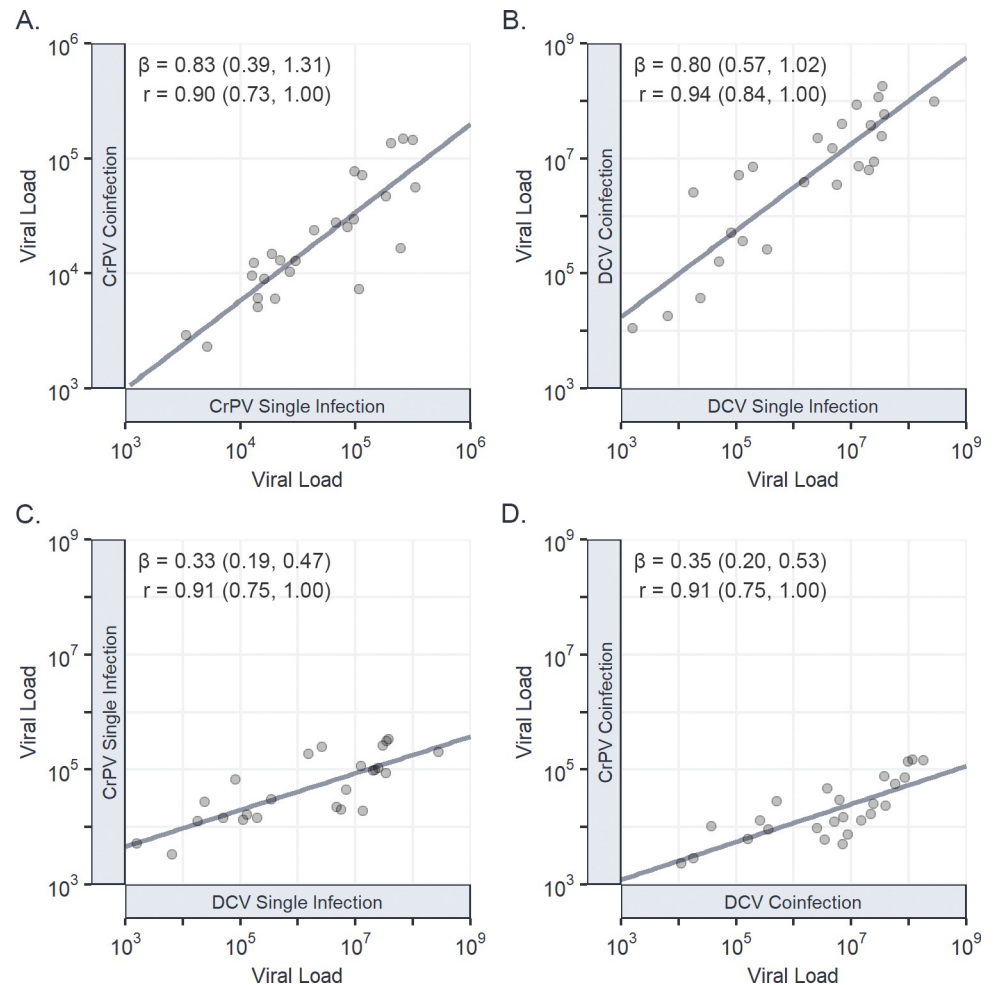


Fig 2. Genetic correlations in viral load between single and coinfections of CrPV and DCV. Correlations in viral load between CrPV during single and coinfection (A); DCV during single and coinfection (B); CrPV and DCV during single infection (C); and CrPV and DCV during coinfection (D). Individual points represent the mean viral load at 2 dpi for each DGRP line on a \log_{10} scale, with trend lines added from a univariate least-squares linear model for illustrative purposes. Genetic correlations (r), regression slopes (β), and 95% CIs have been taken from the output of model (1).

<https://doi.org/10.1371/journal.ppat.1011044.g002>

DCV. The repeatability of viral load across host species was high for both viruses during single infection, CrPV: 0.86 (0.78, 0.93), DCV: 0.94 (0.90, 0.97) and coinfection, CrPV: 0.76 (0.64, 0.87), DCV: 0.89 (0.82, 0.94), with the between-species phylogenetic component explaining a high proportion of the variation in viral load with little within-species variation or measurement error. Although point estimates of these parameters were all consistent with a slight decrease in phylogenetic signal during coinfection, the effect size was small, and we did not detect credible differences in phylogenetic signal between single and coinfection.

Viral load is strongly correlated between single and coinfection across host species

Interspecific correlations in viral load between single and coinfection were calculated for each virus from the variance-covariance matrix of model (4). We found strong positive correlations in viral loads between single and coinfection for DCV: $r = 0.95$ (0.89, 0.99) (Fig 4A) and CrPV:

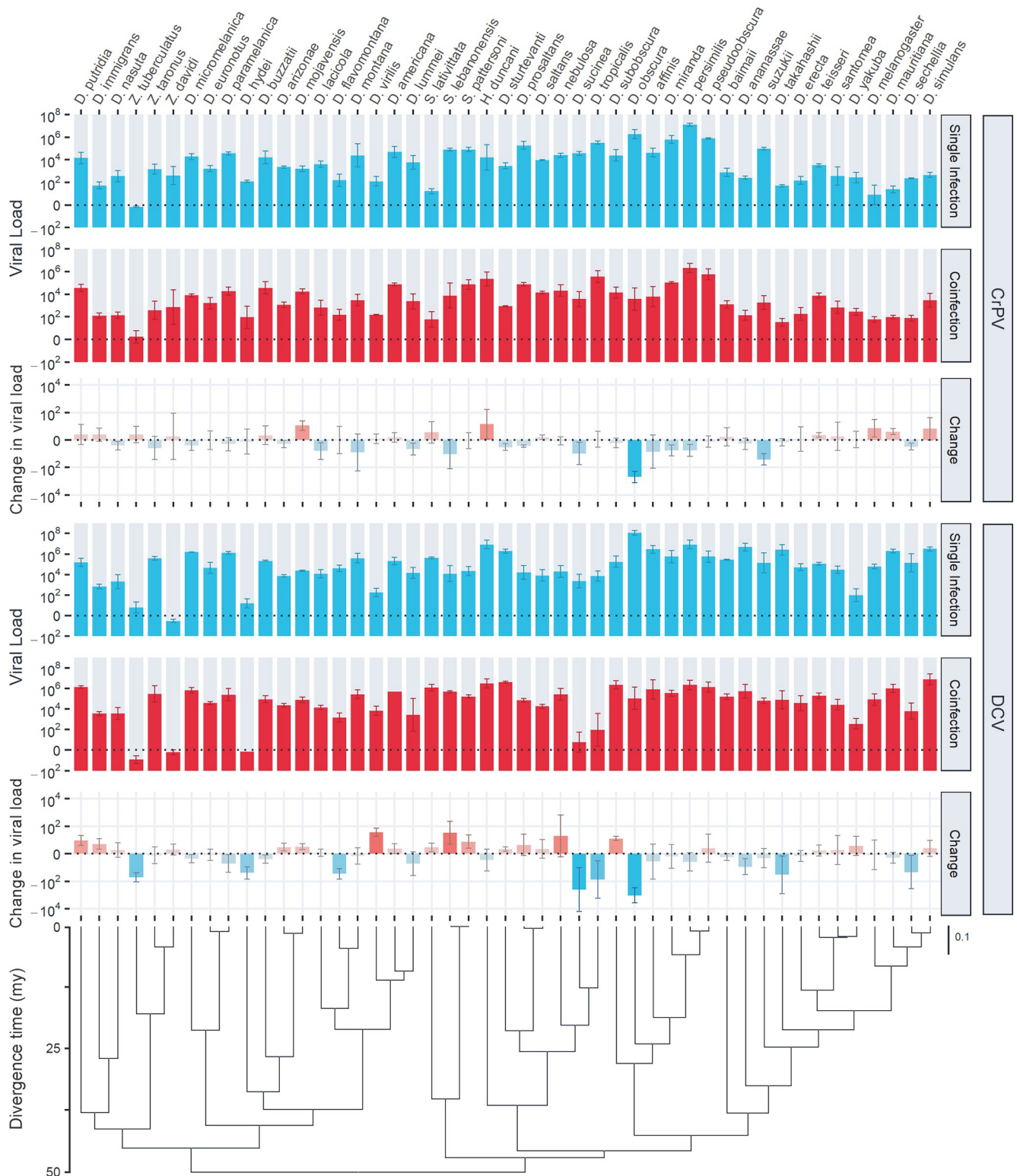


Fig 3. Viral loads of CrPV and DCV across host species during single and coinfection. Bar heights show the mean viral load or changes in viral load (coinfection–single infection) by 2 dpi on a \log_{10} scale, with error bars showing the standard error of the mean. Blue bars represent single infection viral loads, or changes in viral load where single infection viral loads were greater than coinfection. Red bars represent coinfection viral loads, or changes in viral load where coinfection viral loads were greater than single infection. The phylogeny of *Drosophilidae* hosts is presented at the bottom, with the scale bar showing nucleotide substitutions per site, and the axis showing the approximate age since divergence in millions of years (mya) based on estimates from [91].

<https://doi.org/10.1371/journal.ppat.1011044.g003>

Table 2. Estimates of overall mean, across-species variance, repeatability, and the proportion of variance explained by the host phylogeny for viral load and the change in viral load during coinfection. Values for mean viral load, across species variance, and repeatability for the “single infection” and “coinfection” conditions were taken from model (4), which was fitted on \log_{10} -transformed fold-changes in viral load, while these values for “change” during coinfection were taken from model (6), which was fitted on \log_{10} -transformed Δ fold-changes in viral load (coinfection-single infection). The proportion of variance explained by phylogeny was taken from model (3) for the “single infection” and “coinfection” conditions, and model (5) for “change” during coinfection.

Virus	Condition	Mean	Across-species variance	Repeatability	Variance explained by phylogeny
CrPV	Single Infection	3.44 (1.88, 4.99)	3.63 (1.86, 5.75)	0.86 (0.78, 0.93)	0.88 (0.69, 1)
	Coinfection	3.30 (2.21, 4.38)	2.93 (1.36, 4.75)	0.76 (0.64, 0.87)	0.82 (0.82, 1)
	Change	-0.13 (-0.49, 0.19)	0.17 (0, 0.46)	0.11 (0, 0.27)	0.57 (0, 1)
DCV	Single Infection	4.75 (2.09, 7.49)	9.85 (5.20, 15.46)	0.94 (0.90, 0.97)	0.13 (0, 0.43)
	Coinfection	4.57 (1.82, 7.26)	10.40 (4.87, 16.44)	0.89 (0.82, 0.94)	0.10 (0, 0.27)
	Change	-0.12 (-1.08, 0.86)	0.92 (0, 1.84)	0.36 (0.08, 0.62)	0.49 (0, 0.99)

<https://doi.org/10.1371/journal.ppat.1011044.t002>

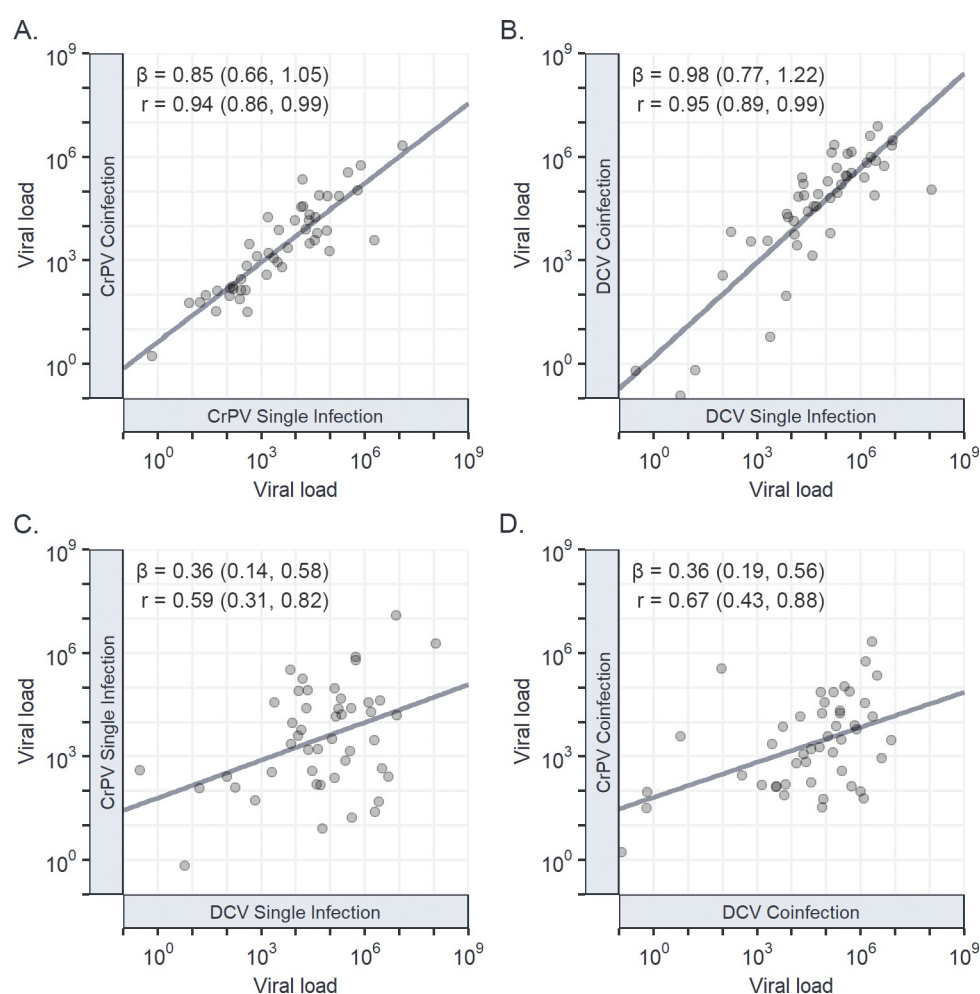


Fig 4. Interspecific correlations in viral load between single and coinfections of CrPV and DCV. Correlations in viral load between CrPV during single and coinfection (A); DCV during single and coinfection (B); CrPV and DCV during single infection (C); and CrPV and DCV during coinfection (D). Individual points represent the mean viral load at 2dpi for each *Drosophilidae* host species on a \log_{10} scale, with trend lines added from a univariate least-squares linear model for illustrative purposes. Interspecific correlations (r), regression slopes (β), and 95% CIs have been taken from the output of model (4).

<https://doi.org/10.1371/journal.ppat.1011044.g004>

$r = 0.94$ (0.86, 0.99) (Fig 4B), with the regression slopes of each indicating a near 1:1 relationship: DCV: $\beta = 0.98$ (0.77, 1.22), CrPV: $\beta = 0.85$ (0.66, 1.05), and limited evidence of host species by coinfection interactions. The strength of the interspecific correlation in viral load between DCV and CrPV (Fig 4C and 4D) also did not differ between single: $r = 0.59$ (0.31, 0.82), and coinfection: $r = 0.67$ (0.43, 0.88) and was consistent with previous estimates: $r = 0.59$ (0.26, 0.87) [42]. As seen within host species, no correlation was detectable between the viral loads of each virus during coinfection and the strength of coinfection interaction experienced by the other virus (S2 Fig), indicating that the strength of coinfection interaction between DCV and CrPV across host species is not virus density dependent.

Little evidence of phylogenetic signal in the strength of coinfection interaction

As the viral loads of DCV and CrPV show a strong phylogenetic signal across host species, we also tested if there was phylogenetic signal across hosts in the change in viral load from single to coinfection (Table 2). Fitting phylogenetic mixed models to these data revealed little support for any phylogenetic signal in the change in viral load during coinfection, with low estimates of repeatability for DCV: 0.36 (0.08, 0.62) and no credible difference from zero for repeatability of CrPV or the variance explained by phylogeny for either virus.

Discussion

Here, we measured variation in the outcome of coinfections within and across host species, using a *Drosophila* experimental system and two *Cripaviruses*: DCV and CrPV. We found effects of coinfection on viral load across genotypes of *D. melanogaster*, with DCV increasing ~3 fold and CrPV decreasing ~2 fold during coinfection. Consistent with previous studies, we found that natural genetic variation explained a large proportion of variation in susceptibility to single infections [65], but little evidence was found for a change in this genetic component of susceptibility in the presence of a coinfecting virus, or for a host genetic component to the strength of interaction between these viruses. Across host species, we found no evidence of consistent coinfection interactions between these viruses and no change in the phylogenetic patterns of susceptibility to each virus during coinfection, although coinfection interactions were apparent in a subset of host species. Strong positive correlations between single and coinfection viral loads, and between DCV and CrPV both within and across host species suggest that similar genetic architectures are underlying susceptibility to these viruses, and that susceptibility is largely independent of coinfection status.

Exploitative coinfection interactions—where one pathogen benefits from coinfection to the detriment of the other—have been described in intestinal parasites of wood mice and wild rabbits [92,93], and in mixed-genotype *Pseudomonas* infections in plants [94]. The mechanisms underlying exploitative coinfection interactions are unknown but may be due to differences in the relative importance of specific interactions between each virus and the host in overall susceptibility. Within *D. melanogaster*, no correlation was seen in the strength of interaction experienced by one virus and the viral loads of the other virus, suggesting that the strength of coinfection interaction is not virus density-dependent, as more susceptible host genotypes did not experience increased changes in viral load with coinfection compared to more resistant genotypes. This suggests that the coinfection interaction within *D. melanogaster* is unlikely to be caused by resource competition between DCV and CrPV, as susceptible hosts experienced >100-fold higher viral loads for both DCV and CrPV compared to more resistant hosts with no evidence of limited virus replication. DCV may instead be benefiting from increased suppression of antiviral RNAi due to expression of the CrPV immune inhibitor [63], while CrPV

is hindered by the activation of other mechanisms of host immunity by DCV. However, complex direct virus-virus interactions have been described in multiple coinfections, and it is possible that DCV and CrPV are directly influencing each other's expression or virion surface composition [19,95].

Across host species, the changes in viral load during coinfection were highly variable and show no consistent interaction between DCV and CrPV. Coupled with the fact we did not detect effects of genetic variation within host species or evolutionary relatedness across host species in the change in viral load during coinfection, our results suggest that natural levels of variation in host genetics have little impact on the strength of interaction between these viruses during coinfection. This contrasts with coinfection studies in other systems, which describe variation between host genotypes in pathogen community composition, coinfection prevalence, and disease severity during coinfection [32–34]. Mathematical models investigating stochasticity during coinfection have suggested that otherwise identical coinfections can have directionally different outcomes [96], and so it may be that any influences of host evolutionary relatedness and genotype are being masked by high stochasticity in the outcome of coinfection in this system. It is possible that stochasticity may be lower in sequential coinfections where the initial virus is able to establish a stable infection before the introduction of a second virus, and a comparison between the stochasticity experienced during simultaneous and sequential coinfection warrants further study. Alternatively, variation in the strength of coinfection interaction between host genotypes may be influenced by a small number of major-effect loci that are not dispersed phylogenetically, which these experiments were not designed to detect. High stochasticity may explain the discrepancy in the direction of coinfection interaction in *D. melanogaster* in our two experiments, where on average CrPV decreases in viral load across DGRP lines but increases in the *D. melanogaster* line used in our across-species experiment (where within-line replicates were lower). However, it is also possible that this change in the direction of interaction is genuine and influenced by the specific genotype of *D. melanogaster* used in the across-species experiment, which was not included in the within-species panel.

As inferential models of cross-species infections grow in complexity, they will continue to incorporate more non-genomic data which is known to influence the outcome of infection (e.g., [97]). Our findings suggest that coinfection will not be a necessary inclusion in models of every host-pathogen system, as the ability of the host phylogeny to explain variation in viral load was largely unaffected during coinfection in this case. Despite this, coinfection is known to cause changes in infection traits in many systems [4–9,98–110], with consequences for pathogen spread and establishment in natural populations [10–15]. Few studies exist that describe pathogens that do not interact during coinfection [111], (although this may represent publication bias), and so the frequency of consequential coinfection interactions in nature is as yet unknown. It remains unclear if interactions between pathogens can be consistently predicted *a priori* from single infection data [112,113], or from pathogen and host genomic data [114]. In cases of direct interaction between pathogens, such as the binding and activation of endogenous HIV by herpes simplex virus proteins [95], differing outcomes in coinfection may be predictable through conventional tools for inferring protein-protein and protein-nucleotide binding [115,116]. However, where pathogens interact indirectly, such as through immune modulation or resource availability, it may be necessary to understand the extent of variation in these host factors that is required to influence the outcome of infection before inferring interactions between coinfecting pathogens.

Here, we have tested for variation in the outcome of coinfection within and across host species, and our findings suggest that host genetics may not influence coinfection interactions in all host-pathogen systems. This approach can now be expanded to a more diverse range of coinfecting pathogens, to look for effects of host genetic variation during other pathogen-

pathogen interactions, to better understand the potential determinants of the outcome of coinfection interactions, and how these interactions may affect the evolution of host susceptibility.

Supporting information

S1 Fig. Correlations within host species between the change in viral load due to coinfection (coinfection viral load—single infection viral load) for CrPV (A) and DCV (B) and the viral loads during coinfection of the opposing virus. Individual points represent the mean viral load or change in viral load at 2 dpi for each DGRP line on a \log_{10} scale, with trend lines added from a univariate least-squares linear model for illustrative purposes. Genetic correlations (r), regression slopes (β), and 95% CIs have been taken from the output of model (1). (DOCX)

S2 Fig. Correlations across host species between the change in viral load due to coinfection (coinfection viral load—single infection viral load) for CrPV (A) and DCV (B) and the viral loads during coinfection of the opposing virus. Individual points represent the mean viral load or change in viral load at 2 dpi for each host species on a \log_{10} scale, with trend lines added from a univariate least-squares linear model for illustrative purposes. Genetic correlations (r), regression slopes (β), and 95% CIs have been taken from the output of model (4). (DOCX)

S1 Methods. Power analysis was used to determine if the level of replication in the across species experiment was sufficient to detect additive effects of coinfection of similar size and variance to those seen in within-species experiments. An additive effect of coinfection was simulated by randomly sampling from normal distributions—generated from the means and variances of changes in viral load across DGRP lines—and adding these values to the single infection viral loads measured across host species. This process was repeated 30 times to produce multiple simulated datasets, which were analysed using phylogenetic GLMMs as described in the main body. The lower 95% credible (HPD) intervals for the estimated changes in viral load during coinfection were examined for each model and consistently showed an ability to detect credible changes in viral load during coinfection of >2-fold across host species.

(DOCX)

S1 Table. DGRP lines. Resistant *pastrel* alleles (G) are coloured orange, and susceptible (A) alleles are coloured blue.

(DOCX)

S2 Table. PCR genotyping primers. Cycle conditions were as follows: initial denaturation at 95°C for 30 seconds; then 10 cycles of 95°C for 15 seconds, 70–60°C (touchdown Δ of -1°C per cycle) for 30 seconds, and 68°C for 60 seconds; then a final extension at 68°C for 5 minutes.

(DOCX)

S3 Table. Drosophilidae host species. * Diets supplemented with additional dry yeast.

(DOCX)

S4 Table. RPL32 primer sequences. Primers were designed to amplify across an intron boundary to ensure only cDNA sequences were amplified. Different primer combinations were used for different host species (see below) to account for SNPs in the primer binding sites.

(DOCX)

S5 Table. RPL32 primer combinations by Drosophilidae species.
(DOCX)

S6 Table. Number of biological replicates (vials of infected flies).
(DOCX)

S7 Table. Heritability (h^2), coefficients of environmental and additive genetic variation (CV_E and CV_A), and evolvability (I_A) of viral load for DCV and CrPV during single and coinfection across DGRP lines. Values were taken from model (1), which was fitted on \log_{10} -transformed fold-changes in viral load.
(DOCX)

S8 Table. Heritability (h^2), coefficients of environmental and additive genetic variation (CV_E and CV_A), and evolvability (I_A) of the change in viral load during coinfection (coinfection—single infection) for DCV and CrPV. Values were taken from model (2), which was fitted on \log_{10} -transformed Δ fold-changes in viral load.
(DOCX)

Acknowledgments

We would like to thank Camille Bonneaud and Ann Tate for useful discussion. For the purpose of Open Access, the author has applied a CC BY public copyright licence to any Author Accepted Manuscript version arising from this submission.

Author Contributions

Conceptualization: Ryan M. Imrie, Katherine E. Roberts, Joanne Lello, Ben Longdon.

Data curation: Ryan M. Imrie, Sarah K. Walsh.

Formal analysis: Ryan M. Imrie, Ben Longdon.

Funding acquisition: Ryan M. Imrie, Ben Longdon.

Investigation: Ryan M. Imrie, Sarah K. Walsh, Katherine E. Roberts.

Methodology: Ryan M. Imrie, Sarah K. Walsh, Katherine E. Roberts, Ben Longdon.

Project administration: Joanne Lello, Ben Longdon.

Supervision: Joanne Lello, Ben Longdon.

Validation: Ryan M. Imrie.

Visualization: Ryan M. Imrie.

Writing – original draft: Ryan M. Imrie.

Writing – review & editing: Ryan M. Imrie, Sarah K. Walsh, Joanne Lello, Ben Longdon.

References

1. Read AF, Taylor LH. The Ecology of Genetically Diverse Infections. *Science*. 2001; 292(5519):1099–102. <https://doi.org/10.1126/science.1059410> PMID: 11352063
2. Petney TN, Andrews RH. Multiparasite communities in animals and humans: frequency, structure and pathogenic significance. *Int J Parasitol*. 1998; 28(3):377–93. [https://doi.org/10.1016/s0020-7519\(97\)00189-6](https://doi.org/10.1016/s0020-7519(97)00189-6) PMID: 9559357
3. Cox FEG. Concomitant infections, parasites and immune responses. *Parasitology*. 2001; 122(S1): S23–38. <https://doi.org/10.1017/s003118200001698x> PMID: 11442193

4. Harrison F, Browning LE, Vos M, Buckling A. Cooperation and virulence in acute *Pseudomonas aeruginosa* infections. *Bmc Biol.* 2006; 4(1):21. <https://doi.org/10.1186/1741-7007-4-21> PMID: 16827933
5. Loving CL, Brockmeier SL, Vincent AL, Palmer MV, Sacco RE, Nicholson TL. Influenza virus coinfection with *Bordetella bronchiseptica* enhances bacterial colonization and host responses exacerbating pulmonary lesions. *Microb Pathogenesis.* 2010; 49(5):237–45. <https://doi.org/10.1016/j.micpath.2010.06.004> PMID: 20558274
6. Karvonen A, Rellstab C, Louhi K-R, Jokela J. Synchronous attack is advantageous: mixed genotype infections lead to higher infection success in trematode parasites. *Proc Royal Soc B Biological Sci.* 2012; 279(1726):171–6. <https://doi.org/10.1098/rspb.2011.0879> PMID: 21632629
7. Kalhoro DH, Gao S, Xie X, Liang S, Luo S, Zhao Y et al. Canine influenza virus coinfection with *Staphylococcus pseudintermedius* enhances bacterial colonization, virus load and clinical presentation in mice. *Bmc Vet Res.* 2016; 12(1):87. <https://doi.org/10.1186/s12917-016-0708-6> PMID: 27259293
8. Lass S, Hudson PJ, Thakar J, Saric J, Harvill E, Albert R et al. Generating super-shedders: co-infection increases bacterial load and egg production of a gastrointestinal helminth. *J Roy Soc Interface.* 2013; 10(80):20120588. <https://doi.org/10.1098/rsif.2012.0588> PMID: 23256186
9. Basso M, Andreis S, Scaggiante R, Franchin E, Zago D, Biasolo MA et al. Cytomegalovirus, Epstein-Barr virus and human herpesvirus 8 salivary shedding in HIV positive men who have sex with men with controlled and uncontrolled plasma HIV viremia: a 24-month longitudinal study. *Bmc Infect Dis.* 2018; 18(1):683. <https://doi.org/10.1186/s12879-018-3591-x> PMID: 30567494
10. Ezenwa VO, Jolles AE. From Host Immunity to Pathogen Invasion: The Effects of Helminth Coinfection on the Dynamics of Microparasites. *Integr Comp Biol.* 2011; 51(4):540–51. <https://doi.org/10.1093/icb/ict058> PMID: 21727178
11. Abu-Raddad LJ, Patnaik P, Kublin JG. Dual Infection with HIV and Malaria Fuels the Spread of Both Diseases in Sub-Saharan Africa. *Science.* 2006; 314(5805):1603–6. <https://doi.org/10.1126/science.1132338> PMID: 17158329
12. Nickbakhsh S, Mair C, Matthews L, Reeve R, Johnson PCD, Thorburn F et al. Virus–virus interactions impact the population dynamics of influenza and the common cold. *P Natl Acad Sci Usa.* 2019; 116(52):27142–50. <https://doi.org/10.1073/pnas.1911083116> PMID: 31843887
13. Mak GC, Wong AH, Ho WYY, Lim W. The impact of pandemic influenza A (H1N1) 2009 on the circulation of respiratory viruses 2009–2011. *Influenza Other Resp.* 2012; 6(3):e6–10. <https://doi.org/10.1111/j.1750-2659.2011.00323.x> PMID: 22212717
14. Xiridou M, Borkent-Raven B, Hulshof J, Wallinga J. How Hepatitis D Virus Can Hinder the Control of Hepatitis B Virus. *Plos One.* 2009; 4(4):e5247. <https://doi.org/10.1371/journal.pone.0005247> PMID: 19381302
15. Farci P, Niro G. Clinical Features of Hepatitis D. *Semin Liver Dis.* 2012; 32(03):228–36. <https://doi.org/10.1055/s-0032-1323628> PMID: 22932971
16. Seppälä O, Jokela J. Do Coinfections Maintain Genetic Variation in Parasites? *Trends Parasitol.* 2016; 32(12):930–8. <https://doi.org/10.1016/j.pt.2016.08.010> PMID: 27614425
17. Garbutt J, Bonsall MB, Wright DJ, Raymond B. Antagonistic competition moderates virulence in *Bacillus thuringiensis*. *Ecol Lett.* 2011; 14(8):765–72. <https://doi.org/10.1111/j.1461-0248.2011.01638.x> PMID: 21635671
18. Bhattacharya A, Díaz VCT, Morran LT, Bashey F. Evolution of increased virulence is associated with decreased spite in the insect-pathogenic bacterium *Xenorhabdus nematophila*. *Biol Letters.* 2019; 15(8):20190432. <https://doi.org/10.1098/rsbl.2019.0432> PMID: 31455168
19. Haney J, Vijayakrishnan S, Streetley J, Dee K, Goldfarb DM, Clarke M et al. Coinfection by influenza A virus and respiratory syncytial virus produces hybrid virus particles. *Nat Microbiol.* 2022; 7(11):1879–90. <https://doi.org/10.1038/s41564-022-01242-5> PMID: 36280786
20. Kümmerli R, Griffin AS, West SA, Buckling A, Harrison F. Viscous medium promotes cooperation in the pathogenic bacterium *Pseudomonas aeruginosa*. *Proc Royal Soc B Biological Sci.* 2009; 276(1672):3531–8. <https://doi.org/10.1098/rspb.2009.0861> PMID: 19605393
21. Ford SA, Kao D, Williams D, King KC. Microbe-mediated host defence drives the evolution of reduced pathogen virulence. *Nat Commun.* 2016; 7(1):13430. <https://doi.org/10.1038/ncomms13430> PMID: 27845328
22. Cressler CE, Nelson WA, Day T, McCauley E, Bonsall M. Disentangling the interaction among host resources, the immune system and pathogens. *Ecol Lett.* 2014; 17(3):284–93. <https://doi.org/10.1111/ele.12229> PMID: 24350974
23. Ramiro RS, Pollitt LC, Mideo N, Reece SE. Facilitation through altered resource availability in a mixed-species rodent malaria infection. *Ecol Lett.* 2016; 19(9):1041–50. <https://doi.org/10.1111/ele.12639> PMID: 27364562

24. Griffiths EC, Fairlie-Clarke K, Allen JE, Metcalf CJE, Graham AL. Bottom-up regulation of malaria population dynamics in mice co-infected with lung-migratory nematodes. *Ecol Lett*. 2015; 18(12):1387–96. <https://doi.org/10.1111/ele.12534> PMID: 26477454
25. Graham AL. Ecological rules governing helminth–microparasite coinfection. *Proc National Acad Sci*. 2008; 105(2):566–70. <https://doi.org/10.1073/pnas.0707221105> PMID: 18182496
26. Modjarrad K, Vermund SH. Effect of treating co-infections on HIV-1 viral load: a systematic review. *Lancet Infect Dis*. 2010; 10(7):455–63. [https://doi.org/10.1016/S1473-3099\(10\)70093-1](https://doi.org/10.1016/S1473-3099(10)70093-1) PMID: 20610327
27. Grivel J-C, Santoro F, Chen S, Fagá G, Malnati MS, Ito Y et al. Pathogenic Effects of Human Herpesvirus 6 in Human Lymphoid Tissue Ex Vivo. *J Virol*. 2003; 77(15):8280–9. <https://doi.org/10.1128/jvi.77.15.8280-8289.2003> PMID: 12857897
28. Lisco A, Grivel J-C, Biancotto A, Vanpouille C, Origgi F, Malnati MS et al. Viral Interactions in Human Lymphoid Tissue: Human Herpesvirus 7 Suppresses the Replication of CCR5-Tropic Human Immunodeficiency Virus Type 1 via CD4 Modulation. *J Virol*. 2007; 81(2):708–17. <https://doi.org/10.1128/jvi.01367-06> PMID: 17065205
29. King CA, Baillie J, Sinclair JH. Human cytomegalovirus modulation of CCR5 expression on myeloid cells affects susceptibility to human immunodeficiency virus type 1 infection. *J Gen Virol*. 2006; 87(8):2171–80. <https://doi.org/10.1099/vir.0.81452-0> PMID: 16847113
30. Biancotto A, Iglehart SJ, Lisco A, Vanpouille C, Grivel J-C, Lurain NS et al. Upregulation of Human Cytomegalovirus by HIV Type 1 in Human Lymphoid Tissue ex Vivo. *Aids Res Hum Retrov*. 2008; 24(3):453–62. <https://doi.org/10.1089/aid.2007.0155> PMID: 18327985
31. Grivel J-C, García M, Moss WJ, Margolis LB. Inhibition of HIV-1 Replication in Human Lymphoid Tissues Ex Vivo by Measles Virus. *J Infect Dis*. 2005; 192(1):71–8. <https://doi.org/10.1086/430743> PMID: 15942896
32. Susi H, Barrès B, Vale PF, Laine A-L. Co-infection alters population dynamics of infectious disease. *Nat Commun*. 2015; 6(1):5975. <https://doi.org/10.1038/ncomms6975> PMID: 25569306
33. Susi H, Laine A. Host resistance and pathogen aggressiveness are key determinants of coinfection in the wild. *Evolution*. 2017; 71(8):2110–9. <https://doi.org/10.1111/evo.13290> PMID: 28608539
34. Sallinen S, Norberg A, Susi H, Laine A-L. Intraspecific host variation plays a key role in virus community assembly. *Nat Commun*. 2020; 11(1):5610. <https://doi.org/10.1038/s41467-020-19273-z> PMID: 33154373
35. Randall J, Cable J, Guschina IA, Harwood JL, Lello J. Endemic infection reduces transmission potential of an epidemic parasite during co-infection. *Proc Royal Soc B Biological Sci*. 2013; 280(1769):20131500. <https://doi.org/10.1098/rspb.2013.1500> PMID: 23966641
36. Lange B, Reuter M, Ebert D, Muylaert K, Decaestecker E. Diet quality determines interspecific parasite interactions in host populations. *Ecol Evol*. 2014; 4(15):3093–102. <https://doi.org/10.1002/ece3.1167> PMID: 25247066
37. van den Berg L, Henneman P, van Dijk KW, Waal HAD de, Oostra BA, Duijn CM van et al. Heritability of dietary food intake patterns. *Acta Diabetol*. 2013; 50(5):721–6. <https://doi.org/10.1007/s00592-012-0387-0> PMID: 22415036
38. Lopez-Minguez J, Dashti HS, Madrid-Valero JJ, Madrid JA, Saxena R, Scheer FAJL et al. Heritability of the timing of food intake. *Clin Nutr*. 2019; 38(2):767–73. <https://doi.org/10.1016/j.clnu.2018.03.002> PMID: 29571565
39. Gilbert GS, Webb CO. Phylogenetic signal in plant pathogen–host range. *Proc National Acad Sci*. 2007; 104(12):4979–83. <https://doi.org/10.1073/pnas.0607968104> PMID: 17360396
40. Longdon B, Hadfield JD, Webster CL, Obbard DJ, Jiggins FM. Host Phylogeny Determines Viral Persistence and Replication in Novel Hosts. *Plos Pathog*. 2011; 7(9):e1002260. <https://doi.org/10.1371/journal.ppat.1002260> PMID: 21966271
41. Longdon B, Hadfield JD, Day JP, Smith SCL, McGonigle JE, Cogni R et al. The Causes and Consequences of Changes in Virulence following Pathogen Host Shifts. *Plos Pathog*. 2015; 11(3):e1004728. <https://doi.org/10.1371/journal.ppat.1004728> PMID: 25774803
42. Imrie RM, Roberts KE, Longdon B. Between virus correlations in the outcome of infection across host species: Evidence of virus by host species interactions. *Evol Lett*. 2021; 5(5):472–83. <https://doi.org/10.1002/evl3.247> PMID: 34621534
43. Roberts KE, Hadfield JD, Sharma MD, Longdon B. Changes in temperature alter the potential outcomes of virus host shifts. *Plos Pathog*. 2018; 14(10):e1007185. <https://doi.org/10.1371/journal.ppat.1007185> PMID: 30339695

44. Longdon B, Day JP, Alves JM, Smith SCL, Houslay TM, McGonigle JE et al. Host shifts result in parallel genetic changes when viruses evolve in closely related species. *Plos Pathog*. 2018; 14(4): e1006951. <https://doi.org/10.1371/journal.ppat.1006951> PMID: 29649296
45. Roberts KE, Longdon B. Viral susceptibility across host species is largely independent of dietary protein to carbohydrate ratios. *J Evolution Biol*. 2021; 34(5):746–56. <https://doi.org/10.1111/jeb.13773> PMID: 33586293
46. Mollentze N, Streicker DG, Murcia PR, Hampson K, Biek R. Virulence mismatches in index hosts shape the outcomes of cross-species transmission. *Proc National Acad Sci*. 2020; 117(46):28859–66. <https://doi.org/10.1073/pnas.2006778117> PMID: 33122433
47. Guth S, Visher E, Boots M, Brook CE. Host phylogenetic distance drives trends in virus virulence and transmissibility across the animal–human interface. *Philosophical Transactions Royal Soc B Biological Sci*. 2019; 374(1782):20190296. <https://doi.org/10.1098/rstb.2019.0296> PMID: 31401961
48. Farrell MJ, Davies TJ. Disease mortality in domesticated animals is predicted by host evolutionary relationships. *Proc National Acad Sci*. 2019; 116(16):201817323. <https://doi.org/10.1073/pnas.1817323116> PMID: 30926660
49. Albery GF, Eskew EA, Ross N, Olival KJ. Predicting the global mammalian viral sharing network using phylogeography. *Nat Commun*. 2020; 11(1):2260. <https://doi.org/10.1038/s41467-020-16153-4> PMID: 32385239
50. Shaw LP, Wang AD, Dylus D, Meier M, Pogacnik G, Dessimoz C et al. The phylogenetic range of bacterial and viral pathogens of vertebrates. *Mol Ecol*. 2020; 29(17):3361–79. <https://doi.org/10.1111/mec.15463> PMID: 32390272
51. Davies TJ, Pedersen AB. Phylogeny and geography predict pathogen community similarity in wild primates and humans. *Proc Royal Soc B Biological Sci*. 2008; 275(1643):1695–701. <https://doi.org/10.1098/rspb.2008.0284> PMID: 18445561
52. Streicker DG, Turmelle AS, Vonhof MJ, Kuzmin IV, McCracken GF, Rupprecht CE. Host Phylogeny Constrains Cross-Species Emergence and Establishment of Rabies Virus in Bats. *Science*. 2010; 329(5992):676–9. <https://doi.org/10.1126/science.1188836> PMID: 20689015
53. Marquis JF, Santos MJ, Teixeira CM, Batista MI, Cabral HN. Host-parasite relationships in flatfish (Pleuronectiformes)—the relative importance of host biology, ecology and phylogeny. *Parasitology*. 2011; 138(1):107–21. <https://doi.org/10.1017/S0031182010001009> PMID: 20819241
54. Carlson CJ, Farrell MJ, Grange Z, Han BA, Mollentze N, Phelan AL et al. The future of zoonotic risk prediction. *Philosophical Transactions Royal Soc B*. 2021; 376(1837):20200358. <https://doi.org/10.1098/rstb.2020.0358> PMID: 34538140
55. Geoghegan JL, Holmes EC. Predicting virus emergence amid evolutionary noise. *Open Biol*. 2017; 7(10):170189. <https://doi.org/10.1098/rsob.170189> PMID: 29070612
56. Hellard E, Fouchet D, Vavre F, Pontier D. Parasite–Parasite Interactions in the Wild: How To Detect Them? *Trends Parasitol*. 2015; 31(12):640–52. <https://doi.org/10.1016/j.pt.2015.07.005> PMID: 26440785
57. Wang X-H, Aliyari R, Li W-X, Li H-W, Kim K, Carthew R et al. RNA Interference Directs Innate Immunity Against Viruses in Adult *Drosophila*. *Science*. 2006; 312(5772):452–4. <https://doi.org/10.1126/science.1125694> PMID: 16556799
58. Galiana-Arnoux D, Dostert C, Schneemann A, Hoffmann JA, Imler J-L. Essential function in vivo for Dicer-2 in host defense against RNA viruses in *drosophila*. *Nat Immunol*. 2006; 7(6):590–7. <https://doi.org/10.1038/ni1335> PMID: 16554838
59. Goto A, Okado K, Martins N, Cai H, Barbier V, Lamielle O et al. The Kinase IKK β Regulates a STING- and NF- κ B-Dependent Antiviral Response Pathway in *Drosophila*. *Immunity*. 2018; 49(2):225–234.e4. <https://doi.org/10.1016/j.immuni.2018.07.013> PMID: 30119996
60. Sansone CL, Cohen J, Yasunaga A, Xu J, Osborn G, Subramanian H et al. Microbiota-Dependent Priming of Antiviral Intestinal Immunity in *Drosophila*. *Cell Host Microbe*. 2015; 18(5):571–81. <https://doi.org/10.1016/j.chom.2015.10.010> PMID: 26567510
61. Costa A, Jan E, Sarnow P, Schneider D. The Imd Pathway Is Involved in Antiviral Immune Responses in *Drosophila*. *Plos One*. 2009; 4(10):e7436. <https://doi.org/10.1371/journal.pone.0007436> PMID: 19829691
62. Rij RP van Saleh M-C, Berry B, Foo C, Houk A, Antoniewski C et al. The RNA silencing endonuclease Argonaute 2 mediates specific antiviral immunity in *Drosophila melanogaster*. *Gene Dev*. 2006; 20(21):2985–95. <https://doi.org/10.1101/gad.1482006> PMID: 17079687
63. Nayak A, Berry B, Tassetto M, Kunitomi M, Acevedo A, Deng C et al. Cricket paralysis virus antagonizes Argonaute 2 to modulate antiviral defense in *Drosophila*. *Nat Struct Mol Biol*. 2010; 17(5):547–54. <https://doi.org/10.1038/nsmb.1810> PMID: 20400949

64. Chtarbanova S, Lamiabie O, Lee K-Z, Galiana D, Troxler L, Meignin C et al. *Drosophila* C Virus Systemic Infection Leads to Intestinal Obstruction. *J Virol*. 2014; 88(24):14057–69. <https://doi.org/10.1128/JVI.02320-14> PMID: 25253354
65. Magwire MM, Fabian DK, Schweyen H, Cao C, Longdon B, Bayer F et al. Genome-Wide Association Studies Reveal a Simple Genetic Basis of Resistance to Naturally Coevolving Viruses in *Drosophila melanogaster*. *Plos Genet*. 2012; 8(11):e1003057. <https://doi.org/10.1371/journal.pgen.1003057> PMID: 23166512
66. Cao C, Cogni R, Barbier V, Jiggins FM. Complex Coding and Regulatory Polymorphisms in a Restriction Factor Determine the Susceptibility of *Drosophila* to Viral Infection. *Genetics*. 2017; 206(4):2159–73. <https://doi.org/10.1534/genetics.117.201970> PMID: 28630113
67. Cogni R, Cao C, Day JP, Bridson C, Jiggins FM. The genetic architecture of resistance to virus infection in *Drosophila*. *Mol Ecol*. 2016; 25(20):5228–41. <https://doi.org/10.1111/mec.13769> PMID: 27460507
68. Martins NE, Faria VG, Nolte V, Schlötterer C, Teixeira L, Sucena É et al. Host adaptation to viruses relies on few genes with different cross-resistance properties. *Proc National Acad Sci*. 2014; 111(16):5938–43. <https://doi.org/10.1073/pnas.1400378111> PMID: 24711428
69. Mackay TFC, Richards S, Stone EA, Barbadilla A, Ayroles JF, Zhu D et al. The *Drosophila melanogaster* Genetic Reference Panel. *Nature*. 2012; 482(7384):173–8. <https://doi.org/10.1038/nature10811> PMID: 22318601
70. Drummond AJ, Suchard MA, Xie D, Rambaut A. Bayesian Phylogenetics with BEAUti and the BEAST 1.7. *Mol Biol Evol*. 2012; 29(8):1969–73. <https://doi.org/10.1093/molbev/mss075> PMID: 22367748
71. Rambaut A, Drummond AJ, Xie D, Baele G, Suchard MA. Posterior Summarization in Bayesian Phylogenetics Using Tracer 1.7. *Systematic Biol*. 2018; 67(5):901–4. <https://doi.org/10.1093/sysbio/syy032> PMID: 29718447
72. Yu G. Using ggtree to Visualize Data on Tree-Like Structures. *Curr Protoc Bioinform*. 2020; 69(1):e96. <https://doi.org/10.1002/cpbi.96> PMID: 32162851
73. Martinez J, Bruner-Montero G, Arunkumar R, Smith SCL, Day JP, Longdon B et al. Virus evolution in Wolbachia-infected *Drosophila*. *Proc Royal Soc B*. 2019; 286(1914):20192117. <https://doi.org/10.1098/rspb.2019.2117> PMID: 31662085
74. Johnson KN, Christian PD. Molecular Characterization of *Drosophila* C Virus Isolates. *J Invertebr Pathol*. 1999; 73(3):248–54. <https://doi.org/10.1006/jipa.1998.4830> PMID: 10222177
75. Johnson KN, Christian PD. A molecular taxonomy for cricket paralysis virus including two new isolates from Australian populations of *Drosophila* (Diptera: Drosophilidae). *Arch Virol*. 1996; 141(8):1509–22. <https://doi.org/10.1007/BF01718251> PMID: 8856030
76. *Drosophila* Ringer's solution. Cold Spring Harbor Protocols. 2007; <https://doi.org/10.1101/pdb.rec10919>
77. Short SM, Lazzaro BP. Female and male genetic contributions to post-mating immune defence in female *Drosophila melanogaster*. *Proc Royal Soc B Biological Sci*. 2010; 277(1700):3649–57. <https://doi.org/10.1098/rspb.2010.0937> PMID: 20573620
78. Duneau DF, Kondolf HC, Im JH, Ortiz GA, Chow C, Fox MA et al. The Toll pathway underlies host sexual dimorphism in resistance to both Gram-negative and Gram-positive bacteria in mated *Drosophila*. *Bmc Biol*. 2017; 15(1):124. <https://doi.org/10.1186/s12915-017-0466-3> PMID: 29268741
79. Schwenke RA, Lazzaro BP. Juvenile Hormone Suppresses Resistance to Infection in Mated Female *Drosophila melanogaster*. *Curr Biol*. 2017; 27(4):596–601. <https://doi.org/10.1016/j.cub.2017.01.004> PMID: 28190728
80. Landum M, Silva MS, Martins N, Teixeira L. Viral route of infection determines the effect of gut bacteria on host resistance and tolerance to disease. *Biorxiv* [Internet]. 2021 Jan 1;2021.02.18.431843. <https://doi.org/10.1101/2021.02.18.431843> Available from: <http://biorxiv.org/content/early/2021/02/18/2021.02.18.431843.abstract>.
81. Ruijter JM, Thygesen HH, Schoneveld OJ, Das AT, Berkhout B, Lamers WH. Factor correction as a tool to eliminate between-session variation in replicate experiments: application to molecular biology and retrovirology. *Retrovirology*. 2006; 3(1):2. <https://doi.org/10.1186/1742-4690-3-2> PMID: 16398936
82. Ruijter JM, Villalba AR, Hellemans J, Untergasser A, Hoff MJB van den. Removal of between-run variation in a multi-plate qPCR experiment. *Biomol Detect Quantification*. 2015; 5:10–4. <https://doi.org/10.1016/j.bdq.2015.07.001> PMID: 27077038
83. Hadfield JD. MCMC Methods for Multi-Response Generalized Linear Mixed Models: The MCMCglmm R Package. *Journal of Statistical Software* [Internet]. 2010; 33(2):1–22. Available from: <http://www.jstatsoft.org/v33/i02/>.

84. Gilchrist GW, Huey RB, Serra L. Rapid evolution of wing size clines in *Drosophila subobscura*. *Genetica*. 2001;112–113(1):273–86. <https://doi.org/10.1023/a:1013358931816> PMID: 11838770
85. Huey RB, Moreteau B, Moreteau J-C, Gibert P, Gilchrist GW, Ives AR et al. Sexual size dimorphism in a *Drosophila* clade, the *D. obscura* group. *Zoology*. 2006; 109(4):318–30. <https://doi.org/10.1016/j.zool.2006.04.003> PMID: 16978850
86. Freckleton RP, Harvey PH, Pagel M. Phylogenetic Analysis and Comparative Data: A Test and Review of Evidence. *Am Nat*. 2002; 160(6):712–26. <https://doi.org/10.1086/343873> PMID: 18707460
87. Hansen TF, Pélabon C, Houle D. Heritability is not Evolvability. *Evol Biol*. 2011; 38(3):258. <https://doi.org/10.1007/s11692-011-9127-6>
88. Pagel M. Inferring the historical patterns of biological evolution. *Nature*. 1999; 401(6756):877–84. <https://doi.org/10.1038/44766> PMID: 10553904
89. Housworth EA, Martins EP, Lynch M. The Phylogenetic Mixed Model. *Am Nat*. 2004; 163(1):84–96. <https://doi.org/10.1086/380570> PMID: 14767838
90. Falconer D. Introduction to quantitative genetics. 4th ed. Pearson Education India; 1996.
91. Kim BY, Wang JR, Miller DE, Barmina O, Delaney E, Thompson A et al. Highly contiguous assemblies of 101 drosophilid genomes. *Elife*. 2021; 10:e66405. <https://doi.org/10.7554/eLife.66405> PMID: 34279216
92. Clerc M, Devevey G, Fenton A, Pedersen AB. Antibodies and coinfection drive variation in nematode burdens in wild mice. *Int J Parasitol*. 2018; 48(9–10):785–92. <https://doi.org/10.1016/j.ijpara.2018.04.003> PMID: 29920254
93. Lello J, Boag B, Fenton A, Stevenson IR, Hudson PJ. Competition and mutualism among the gut helminths of a mammalian host. *Nature*. 2004; 428(6985):840–4. <https://doi.org/10.1038/nature02490> PMID: 15103373
94. Barrett LG, Bell T, Dwyer G, Bergelson J. Cheating, trade-offs and the evolution of aggressiveness in a natural pathogen population. *Ecol Lett*. 2011; 14(11):1149–57. <https://doi.org/10.1111/j.1461-0248.2011.01687.x> PMID: 21951910
95. Perre PV de, Segondy M, Foulongne V, Ouedraogo A, Konate I, Huraux J-M et al. Herpes simplex virus and HIV-1: deciphering viral synergy. *Lancet Infect Dis*. 2008; 8(8):490–7. [https://doi.org/10.1016/S1473-3099\(08\)70181-6](https://doi.org/10.1016/S1473-3099(08)70181-6) PMID: 18652995
96. Pinky L, Gonzalez-Parra G, Dobrovolny HM. Effect of stochasticity on coinfection dynamics of respiratory viruses. *Bmc Bioinformatics*. 2019; 20(1):191. <https://doi.org/10.1186/s12859-019-2793-6> PMID: 30991939
97. Brierley L, Pedersen AB, Woolhouse MEJ. Tissue tropism and transmission ecology predict virulence of human RNA viruses. *Plos Biol*. 2019; 17(11):e3000206. <https://doi.org/10.1371/journal.pbio.3000206> PMID: 31770368
98. Brealey JC, Chappell KJ, Galbraith S, Fantino E, Gaydon J, Tozer S et al. *Streptococcus pneumoniae* colonization of the nasopharynx is associated with increased severity during respiratory syncytial virus infection in young children. *Respirol Carlton Vic*. 2018; 23(2):220–7. <https://doi.org/10.1111/resp.13179> PMID: 28913912
99. Garcia-Garcia ML, Calvo C, Ruiz S, Pozo F, Pozo V del, Remedios L et al. Role of viral coinfections in asthma development. *Plos One*. 2017; 12(12):e0189083. <https://doi.org/10.1371/journal.pone.0189083> PMID: 29206851
100. Waknine-Grinberg JH, Gold D, Ohayon A, Flescher E, Heyfets A, Doenhoff MJ et al. *Schistosoma mansoni* infection reduces the incidence of murine cerebral malaria. *Malaria J*. 2010; 9(1):5–5. <https://doi.org/10.1186/1475-2875-9-5> PMID: 20051114
101. Yoshida L-M, Suzuki M, Nguyen HA, Le MN, Vu TD, Yoshino H et al. Respiratory syncytial virus: coinfection and paediatric lower respiratory tract infections. *Eur Respir J*. 2013; 42(2):461–9. <https://doi.org/10.1183/09031936.00101812> PMID: 23645407
102. Bo-shun Z, Li L, Qian Z, Zhen W, Peng Y, Guo-dong Z et al. Co-infection of H9N2 influenza virus and *Pseudomonas aeruginosa* contributes to the development of hemorrhagic pneumonia in mink. *Vet Microbiol*. 2020; 240:108542. <https://doi.org/10.1016/j.vetmic.2019.108542> PMID: 31902499
103. Pomorska-Mól M, Dors A, Kwit K, Kowalczyk A, Stasiak E, Pejsak Z. Kinetics of single and dual infection of pigs with swine influenza virus and *Actinobacillus pleuropneumoniae*. *Vet Microbiol*. 2017; 201:113–20. <https://doi.org/10.1016/j.vetmic.2017.01.011> PMID: 28284596
104. Bandilla M, Valtanen ET, Suomalainen L-R, Aphalo PJ, Hakalahti T. A link between ectoparasite infection and susceptibility to bacterial disease in rainbow trout. *Int J Parasitol*. 2006; 36(9):987–91. <https://doi.org/10.1016/j.ijpara.2006.05.001> PMID: 16750536
105. Righetti AA, Glinz D, Adiossan LG, Koua A-YG, Niamké S, Hurrell RF et al. Interactions and Potential Implications of *Plasmodium falciparum*-Hookworm Coinfection in Different Age Groups in South-

- Central Côte d'Ivoire. *Plos Neglect Trop D*. 2012; 6(11):e1889. <https://doi.org/10.1371/journal.pntd.0001889> PMID: 23133691
106. Mahana O, Arafa A-S, Erfan A, Hussein HA, Shalaby MA. Pathological changes, shedding pattern and cytokines responses in chicks infected with avian influenza-H9N2 and/or infectious bronchitis viruses. *Virusdisease*. 2019; 30(2):279–87. <https://doi.org/10.1007/s13337-018-00506-1> PMID: 31179367
 107. Fondong VN, Pita JS, Rey MEC, Kochko A de, Beachy RN, Fauquet CM. Evidence of synergism between African cassava mosaic virus and a new double-recombinant geminivirus infecting cassava in Cameroon. *J Gen Virol*. 2000; 81(1):287–97. <https://doi.org/10.1099/0022-1317-81-1-287> PMID: 10640569
 108. Clerc M, Fenton A, Babayan SA, Pedersen AB. Parasitic nematodes simultaneously suppress and benefit from coccidian coinfection in their natural mouse host. *Parasitology*. 2019; 146(8):1096–106. <https://doi.org/10.1017/S0031182019000192> PMID: 30915927
 109. Péréfarres F, Thébaud G, Lefeuvre P, Chiroleu F, Rimbaud L, Hoareau M et al. Frequency-dependent assistance as a way out of competitive exclusion between two strains of an emerging virus. *Proc Royal Soc B Biological Sci*. 2014; 281(1781):20133374. <https://doi.org/10.1098/rspb.2013.3374> PMID: 24598426
 110. Salines M, Barnaud E, Andraud M, Eono F, Renon P, Bourry O et al. Hepatitis E virus chronic infection of swine co-infected with Porcine Reproductive and Respiratory Syndrome Virus. *Vet Res*. 2015; 46(1):55. <https://doi.org/10.1186/s13567-015-0207-y> PMID: 26048774
 111. Andersson M, Scherman K, Råberg L. Multiple-Strain Infections of *Borrelia afzelii*: A Role for Within-Host Interactions in the Maintenance of Antigenic Diversity? *Am Nat*. 2013; 181(4):545–54. <https://doi.org/10.1086/669905> PMID: 23535618
 112. Lello J, McClure SJ, Tyrrell K, Viney ME. Predicting the effects of parasite co-infection across species boundaries. *Proc Royal Soc B Biological Sci*. 2018; 285(1874):20172610. <https://doi.org/10.1098/rspb.2017.2610> PMID: 29540516
 113. Lello J, Hussell T. Functional group/guild modelling of inter-specific pathogen interactions: A potential tool for predicting the consequences of co-infection. *Parasitology*. 2008; 135(7):825–39. <https://doi.org/10.1017/S0031182008000383> PMID: 18477416
 114. Fenton A, Viney ME, Lello J. Detecting interspecific macroparasite interactions from ecological data: patterns and process. *Ecol Lett*. 2010; 13(5):606–15. <https://doi.org/10.1111/j.1461-0248.2010.01458.x> PMID: 20529102
 115. Yan J, Friedrich S, Kurgan L. A comprehensive comparative review of sequence-based predictors of DNA- and RNA-binding residues. *Brief Bioinform*. 2015; 17(1):88–105. <https://doi.org/10.1093/bib/bbv023> PMID: 25935161
 116. Keskin O, Tuncbag N, Gursoy A. Predicting Protein–Protein Interactions from the Molecular to the Proteome Level. *Chem Rev*. 2016; 116(8):4884–909. <https://doi.org/10.1021/acs.chemrev.5b00683> PMID: 27074302